NASA/TM—2000-209931 AIAA–2000–0570

Quasi-Steady Acceleration Direction Indicator in Three Dimensions

Richard DeLombard, Emily S. Nelson and Kenol Jules
Glenn Research Center, Cleveland, Ohio

May 2000

The NASA STI Program Office . . . in Profile

Since its founding, NASA has been dedicated to the advancement of aeronautics and space science. The NASA Scientific and Technical Information (STI) Program Office plays a key part in helping NASA maintain this important role.

The NASA STI Program Office is operated by Langley Research Center, the Lead Center for NASA's scientific and technical information. The NASA STI Program Office provides access to the NASA STI Database, the largest collection of aeronautical and space science STI in the world. The Program Office is also NASA's institutional mechanism for disseminating the results of its research and development activities. These results are published by NASA in the NASA STI Report Series, which includes the following report types:

- TECHNICAL PUBLICATION. Reports of completed research or a major significant phase of research that present the results of NASA programs and include extensive data or theoretical analysis. Includes compilations of significant scientific and technical data and information deemed to be of continuing reference value. NASA's counterpart of peer-reviewed formal professional papers but has less stringent limitations on manuscript length and extent of graphic presentations.

- TECHNICAL MEMORANDUM. Scientific and technical findings that are preliminary or of specialized interest, e.g., quick release reports, working papers, and bibliographies that contain minimal annotation. Does not contain extensive analysis.

- CONTRACTOR REPORT. Scientific and technical findings by NASA-sponsored contractors and grantees.

- CONFERENCE PUBLICATION. Collected papers from scientific and technical conferences, symposia, seminars, or other meetings sponsored or cosponsored by NASA.

- SPECIAL PUBLICATION. Scientific, technical, or historical information from NASA programs, projects, and missions, often concerned with subjects having substantial public interest.

- TECHNICAL TRANSLATION. English-language translations of foreign scientific and technical material pertinent to NASA's mission.

Specialized services that complement the STI Program Office's diverse offerings include creating custom thesauri, building customized data bases, organizing and publishing research results . . . even providing videos.

For more information about the NASA STI Program Office, see the following:

- Access the NASA STI Program Home Page at ***http://www.sti.nasa.gov***

- E-mail your question via the Internet to help@sti.nasa.gov

- Fax your question to the NASA Access Help Desk at (301) 621-0134

- Telephone the NASA Access Help Desk at (301) 621-0390

- Write to:
  NASA Access Help Desk
  NASA Center for AeroSpace Information
  7121 Standard Drive
  Hanover, MD 21076

NASA/TM—2000-209931 AIAA–2000–0570

Quasi-Steady Acceleration Direction Indicator in Three Dimensions

Richard DeLombard, Emily S. Nelson and Kenol Jules
Glenn Research Center, Cleveland, Ohio

Prepared for the
38th Aerospace Sciences Meeting and Exhibit
sponsored by the American Institute of Aeronautics and Astronautics
Reno, Nevada, January 10–13, 2000

National Aeronautics and
Space Administration

Glenn Research Center

May 2000

This report contains preliminary findings, subject to revision as analysis proceeds.

Available from

NASA Center for Aerospace Information
7121 Standard Drive
Hanover, MD 21076
Price Code: A03

National Technical Information Service
5285 Port Royal Road
Springfield, VA 22100
Price Code: A03

QUASI-STEADY ACCELERATION DIRECTION INDICATOR IN THREE DIMENSIONS

Richard DeLombard, Emily S. Nelson, and Kenol Jules
National Aeronautics and Space Administration
Glenn Research Center
Cleveland, Ohio 44135

ABSTRACT

Many materials processing and fluids physics experiments conducted in a microgravity environment require knowledge of the orientation of the low-frequency acceleration vector. This need becomes especially acute for space experiments such as directional solidification of a molten semiconductor, which is extremely sensitive to orientation and may involve tens of hours of operations of a materials furnace. These low-frequency acceleration data have been measured for many Shuttle missions with the Orbital Acceleration Research Experiment. Previous attempts at using fluid chambers for acceleration measurements have met with limited success due to pointing and vehicle attitude complications. An acceleration direction indicator is described, which is comprised of two orthogonal short cylinders of fluid, each with a small bubble. The motion and the position of the bubble within the chamber will indicate the direction of the acceleration experienced at the sensor location. The direction of the acceleration vector may then be calculated from these data. The frequency response of such an instrument may be tailored for particular experiments with the proper selection of fluid and gas parameters, surface type, and geometry. A three-dimensional system for sensing and displaying the low-frequency acceleration direction via an innovative technique described in this paper has advantages in terms of size, mass, and power compared with electronic instrumentation systems.

Glossary of Terms

D	characteristic length
g	acceleration magnitude
R_c	chamber radius
R_b	bubble radius
r	radial position of bubble
R_e	Reynolds number
R'	radial position of bubble center at wall, $R' = R_c - R_b$
U	characteristic velocity
V_b	bubble velocity
V_{b_t}	bubble terminal velocity
v_f	kinematic viscosity of liquid
α	acceleration angular direction change, $\alpha = \lvert\theta_f - \theta_i\rvert$
β	angle at which freely moving bubble is constrained by the chamber wall
θ_b	angular position of bubble
θ_i	initial position of bubble
θ_f	equilibrium position of bubble
μ_f	dynamic viscosity of liquid
ρ_b	density of bubble
ρ_f	density of liquid

INTRODUCTION

The microgravity acceleration environment can be captured in its full richness and complexity using a variety of acceleration instruments. But while microgravity acceleration data are essential to virtually every space experiment, each individual experiment may only require a subset of that complete data set, such as detailed acceleration magnitude data in particular frequency bands. For problems such as directional solidification of a semiconductor, the orientation of the net acceleration vector relative to the sample is critical. Off-axis orientation of the acceleration can give rise to substantial convective flow due to the large density gradients in the melt. For this problem in a space laboratory under normal operating conditions, knowledge of the orientation of the acceleration with respect to time may be of more importance than the magnitude.

The proposed Quasi-steady Acceleration Direction Indicator device will provide such data in real time with low power requirements, low mass, small volume, and low cost.

PREVIOUS SYSTEMS

The Passive Accelerometer System[1] flown on USML-1 used a spherical ball in a fluid-filled long cylinder to measure the acceleration magnitude based on the ball's speed through the chamber. Limitations of restricted vehicle attitude and constrained instrument pointing have made this device difficult to use for long periods of time. Since this instrument was pointed manually by the crew, the vehicle attitude stability was important. If the vehicle attitude changed, the device had to be re-aligned manually by the crew.

For some materials processing experiments[2], the axial to normal acceleration ratio was used as a measure of the quality of the microgravity environment for the experiment.[3] The axial to normal acceleration ratio is the ratio of the component of the acceleration vector aligned with the long axis of the sample (the axial component) to the component of the acceleration vector acting perpendicular to the sample's long axis (the normal component). The goal during experiment operations was to maximize the axial to normal ratio, which is to say that the quasi-steady acceleration is more aligned with the sample. On several Shuttle microgravity missions, Principal Investigators requested that the attitude of the Shuttle be established in such a way as to maximize this ratio during experiment operations.

INSTRUMENT DESIGN

The Quasi-steady Acceleration Direction Indicator is comprised of two short, orthogonal, right-cylindrical chambers filled with a fluid, figure 1. Inside the liquid is a small bubble with a volume of approximately 5%, relative to the chamber volume. When exposed to the microgravity environment, the bubble's position within the chamber is controlled by the quasi-steady acceleration and fluid wall effect forces.

The frequency response of the bubble motion is dependent on the fluid viscosity, relative bubble size, and the chamber depth vs. width ratio.

ANALYSIS OF BUBBLE MOTION IN MICROGRAVITY

To investigate the response of the Quasi-steady Acceleration Direction Indicator, a step change in the orientation of acceleration is considered. With such a change, there are three modes of motion of the bubble from an initial location to a final, stable location. The first path is a constrained motion along a curved wall, figure 2. The second path is illustrated by path 1 of figure 3 as a free motion through the liquid without being constrained by the walls. The third is a combination of constrained and free motion, paths 1 and 2 of figure 3.

Several assumptions made for a numeric model of the Quasi-steady Acceleration Direction Indicator are:

1) the Reynolds number remains much less than one, $R_e \ll 1$, where $R_e = (UD)/\nu_f$,
2) the bubble remains spherical,
3) the magnitude of the acceleration remains roughly constant, and
4) the effects of liquid flow driven by the chamber walls and any surface tension effects at the wall are ignored.

Performing a force balance for the bubble leads to an expression for the acceleration of the bubble when exposed to an acceleration, g.

$$\frac{dV_b}{dt} = \left(\frac{\rho_f}{\rho_b} - 1\right)g - \frac{3\mu_f V_b}{\rho_b R_b^2} \qquad (1)$$

At the terminal velocity, V_{b_t}, acceleration and drag forces balance, so that

$$\frac{dV_b}{dt} = 0.$$

The terminal velocity is then

$$V_{b_t} \cong \frac{1}{3}\left(\frac{R_b^2 g}{\nu_f}\right). \qquad (2)$$

For this configuration and velocity,

$$Re = 10^{-4} \ll 1.$$

Therefore, in a step-wise calculation with *n* denoting an iteration number, the velocity is given by

$$V_b^{n+1} = min(V_b^n + \frac{dV_b^n}{dt}\Delta t, V_{b_t}). \qquad (3)$$

We have based our calculations on an off-the-shelf fluid level sensor. The chamber, of radius R_c = 1.3 cm, is filled with water and an air bubble with a radius R_b of approximately 3.5 mm. The system is subjected to an acceleration of 1 μg with various step changes in orientation. For a bubble which is free within the fluid, the bubble achieves 99% V_{b_t} at about 0.02 sec. after having traveled 0.00007 cm. The time step chosen for the calculations presented below was 0.1 milliseconds. A free bubble in the chamber may travel as far as $2R' = 1.9cm$, which requires 468 seconds. In many

typical scenarios, the freely moving bubble will be moving through the fluid at terminal velocity.

Constrained bubble motion

When motion of the bubble is constrained by the wall, the position of the bubble is shown in figures 2 and 4 and defined by:

$$r = R' = R_c - R_b \text{ and} \tag{4}$$

$$|\alpha| = |\theta_f - \theta_i| \le \frac{\pi}{2}. \tag{5}$$

Only the tangential acceleration component drives the bubble motion, so that the g in equations (1) and (2) is reduced to the tangential component, $g \cdot \sin(\theta_f - \theta_b)$.

The new bubble position after a small time increment, Δt, is:

$$r_b^{n+1} = R' \tag{6}$$

$$\theta_b^{n+1} = \theta_b + \frac{V_b^{n+1}\Delta t}{R'}. \tag{7}$$

In cartesian coordinates, the position is given by:

$$\vec{b} = (R'\cos\theta_b^{n+1},\ R'\sin\theta_b^{n+1}). \tag{8}$$

The effect of the wall is clearly evident in figure 5 for $\theta_f - \theta_i = \pi/2$, which shows the azimuthal position of the bubble as a function of time. The tangential acceleration component decreases towards zero as the bubble approaches its equilibrium position, resulting in an asymptotic approach to θ_f. The bubble reaches 99% θ_f in about 1648 seconds. We expect that, on the International Space Station, the change in quasi-steady acceleration over an orbit of approximately 5400 seconds will be no more than 54 degrees and most likely significantly smaller. Moreover, the quasi-steady acceleration variation is much more gentle than the case considered here. For $\theta_f - \theta_i = 54$ degrees, the bubble reaches 99% of its equilibrium position at 1489 seconds (which may be a needlessly conservative estimate). For step changes on the order of 10 degrees, the response time is reduced to 1078 seconds.

Free bubble motion

For a bubble away from the chamber wall, the bubble motion direction is determined by the acceleration vector direction.

For a bubble against the chamber wall at the initiation of an acceleration step change with $\pi/2 < |\alpha| \le \pi$, the bubble moves away from the wall and continues freely through the liquid until contacting the wall again. Free motion through the liquid means that one of the following is true:

$$r < R' = R_c - R_b$$

or

$$\frac{\pi}{2} < |\alpha| < \pi.$$

The distance travelled by the bubble over a time step, Δt is:

$$d(n+1) = V_b^{n+1}\Delta t.$$

The coordinates for the new bubble position are given by:

$$x_b^{n+1} = x_b^n + d\cos(\theta_f - \theta_b^n), \tag{9}$$

$$y_b^{n+1} = y_b^n + d\sin(\theta_f - \theta_b^n), \tag{10}$$

$$b^{n+1} = \sqrt{(x_b^{n+1})^2 + (y_b^{n+1})^2}, \text{ and} \tag{11}$$

$$\theta_b^{n+1} = \operatorname{atan}\left(\frac{y_b^{n+1}}{x_b^{n+1}}\right) \tag{12}$$

The bubble reaches the wall at an angle of

$$\beta = 2\left(\alpha - \frac{\pi}{2}\right).$$

At this point, the bubble is constrained by the wall, and the calculation of bubble position with time proceeds using the analysis for a confined bubble above.

Although it is unlikely that a severe step change of the sort described here will be realized on the International Space Station, we have also examined many of these scenarios. An example is shown in figure 6, documenting the azimuthal position history for $\theta_f - \theta_i = 160°$. The bubble lifts off from its resting position at $\theta_i = 0$ in the direction of θ_f. The bubble meets the chamber wall at $\theta_w = 140$ degrees. Note that there is a significant period during which the bubble travels relatively speedily at terminal velocity. Its motion slows down, as expected, once it is confined by the wall. It reaches 99% θ_f at 1682 seconds.

The choice of chamber and bubble geometry and the fluids used can decrease the response time, as deemed necessary.

Prototype

An initial prototype, figure 1, was fabricated for use in the NASA Glenn Research Center 2.2 second drop tower. The prototype contained two commercial bubble levels in an orthogonal orientation with a mirror at 45°. This arrangement allowed both bubble levels to be observed simultaneously with a single camera.

The 2.2 second drop tower[4] utilizes an experiment carrier within a drag shield enclosure to minimize aerodynamic drag accelerations on the experiment carrier. Under normal operations, the experiment carrier, inside the top of the drag shield, is released so the experiment carrier falls clear of the drag shield until the landing at the bottom. The drag shield enclosure is decelerated due to the aerodynamic drag and so the experiment carrier inside gradually falls to the bottom of the drag shield.

The prototype was dropped initially with the experiment carrier attached to the drag shield so as to experience a slight acceleration level due to the aerodynamic drag. During the test, the drag shield and the experiment carrier experienced an increasing acceleration due to the increasing velocity through the air. Initially, the bubble in the vertical plane was at the top of the chamber due to gravity. As soon as the carrier was released to fall, the bubble was observed to move toward the center of the indicator but remained above the outer ring of the indicator, figure 7a. The bubble on the horizontal surface remained in the same approximate position during the drop. This captive test was repeated four times with similar results each time.

The prototype was then dropped in the free fall condition with the experiment carrier separate from the drag shield to minimize the aerodynamic drag on the experiment carrier. Initially, the bubble on the vertical two-dimensional indicator chamber was at the top of the chamber due to gravity. As soon as the carrier was released to fall, the bubble was observed to move toward the center of the indicator and crossed the outer ring of the indicator, figure 7b. The bubble on the horizontal surface remained in the same approximate position during the drop. This free fall test was repeated three times with similar results each time.

When the payload is released in the drop tower, the system undergoes a marked step change in its acceleration magnitude, although the primary component of the acceleration is still vertically down. Some off-axis jitter is present and may be appreciable. The delicate balance of the bubble weight and buoyancy of the bubble, the fluid inertia, and the surface tension force due to bubble distortion and the available area for wetting is severely disrupted. We would expect that the higher-density preferentially wetting water may result in significant fluid flows as a result of the impulsive variation in acceleration and the variation in density between the two fluids. The precise quantification of the forces involved can not be captured in a simple numerical analysis such as is presented here. The front-to-back separation at the edge of the chamber, which is less than the bubble diameter, causes the bubble to form a resting oblate shape at 1g, as depicted in Figure 8. As the bubble moves downward after the drop, the front-to-back separation in the chamber relaxes, allowing the surface tension forces to create a spherically shaped bubble. We expect that as the hydrostatic and dynamic pressures equilibrate in the chamber, the bubble would move back up to the top of the chamber. If the bubble moves down to 0.40 *R'*, buoyant forces would require about 187 seconds to bring the bubble back up to its equilibrium position at the top of the chamber, much longer than is allowed in the experiment.

This centering action provided by the tapered chamber thickness at the edges is not desired for a microgravity device. The chamber would be fabricated with parallel front and back surfaces and a separation distance greater than the bubble diameter.

IMPLEMENTATION

Data acquisition and analysis

Data acquisition may be accomplished by video captured at a prescribed rate, depending on the desired frequency response. For low-frequency response, the frame rate would be quite slow relative to standard video and therefore could conceivably be sent to a ground station by interleaving in other video data streams.

The bubble position can be determined frame-by-frame by a computer image processing algorithm which would detect the bubble edges and calculate the bubble centroid location. To evaluate this concept, these data will be compared with data measured with a low-frequency accelerometer.

Enhancements and options

The basic concepts of the Quasi-steady Acceleration Direction Indicator may be applied in several different ways which will be explored in the future. Using transparent containers, these cylindrical chambers may be stacked so that more than one chamber/bubble combination may be observed simultaneously. This

would allow two (or more) chambers with different response characteristics to be observed simultaneously.

Alternately, a bubble with specific gravity less than the fluid and a particle with a specific gravity greater than the fluid could be combined in one chamber.

ISS MICROGRAVITY ENVIRONMENT

Requirements for environment

The requirements imposed on the ISS vehicle during microgravity mode operations include constraints on the amount of acceleration to which the science experiments are exposed. These requirements are documented in the System Specification for Space Station[5] and include quasi-steady ($f \leq 0.01$ Hz), vibratory ($0.01 < f < 300$ Hz), and transient acceleration constraints. These requirements apply to 50 percent of the internal payload locations. The constraints at the centers of those internal payload locations are stated such that the quasi-steady acceleration:

1) magnitude is less than or equal to 1 μg, and
2) the component perpendicular to the orbital average acceleration vector is less than or equal to 0.2 μg.

This defines a cylinder of radius 0.2 μg and of length 2 μg, within which the instantaneous acceleration vector must lie. This means that while the acceleration magnitude is constrained, the angle variation measured relative to the orbital average vector is unconstrained.

Predicted environment

The ISS Program prepares analytical predictions of the ISS microgravity environment in their Design Analysis Cycles (DAC). Analytical results[6] show that the maximum angle deviation from the orbital average is approximately 27 degrees for racks in the ceiling of the U.S. Laboratory module after the ISS assembly is complete. More stable results are predicted for the port and starboard racks which should have a maximum deviation of only 7 degrees. The ceiling rack location results imply a worst case deviation of +/-27 degrees over one orbit, which must be adequately measured by the Quasi-steady Acceleration Direction Indicator.

Once a stable position has been attained by a Quasi-steady Acceleration Direction Indicator, the maximum deviation (54 degrees) for one orbit should keep the bubble constrained against the chamber wall.

FUTURE WORK

The theoretical analysis presented above did not account for the flows generated in the chamber by the motion of the bubble itself or by an impulsive change in acceleration magnitude. We expect to incorporate these features into our understanding of the problem by numerical simulation using the latest version of FIDAP (v. 8.5.2).

We also intend to investigate the impact of the chamber geometry, the bubble size, and the thermo-physical properties of the fluids involved to optimize the sensor design. Conditions of oscillatory and transient accelerations will be investigated also.

CONCLUSIONS

The Quasi-steady Acceleration Direction Indicator appears to be a reasonable approach for acquiring low-frequency acceleration direction information for microgravity experiments on the International Space Station.

REFERENCES

[1] Matisak, B. P., Rogers, M. J. B., and Alexander, J. I. D.: Analysis of the Passive Accelerometer System (PAS) Measurements During USML-1, AIAA94-0434 (1004)

[2] Arnold, W., Jacqmin, D., Gaug, R., and Chait, A.: Three-dimensional flow transport modes in directional solidification during space processing, J. Spacecraft and Rockets 28:238-243, 1991.

[3] Matisak, B. P., Zhao, A. X., Narayanan, R., and Fripp, A. L.: The microgravity environment: its prediction, measurement, and importance to materials processing, J. of Crystal Growth 174, pp 90-95, 1997.

[4] Lekan, J., Gotti, D. J., Jenkins, A. J., Owens, J. C., and Johnston, M. R.: Users Guide for the 2.2 Second Drop Tower of the NASA Lewis Research Center, NASA Technical Memorandum 107090, April 1996.

[5] International Space Station Program: System Specification for Space Station, SSP 41000.

[6] Laible, M., Quasi-steady Microgravity Analysis, 18th Microgravity Measurements Group meeting, Cocoa Beach, Florida, June 1999.

Figure 1: Prototype Quasi-steady Acceleration Direction Indicator for drop tower tests.

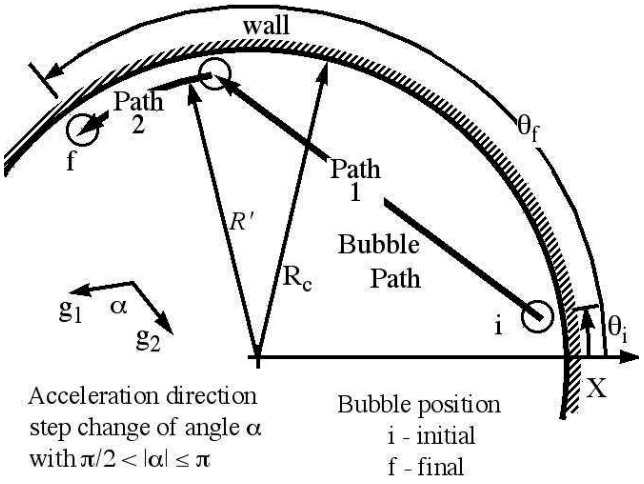

Figure 3: Bubble path for acceleration direction step changes between 90° and 180°.

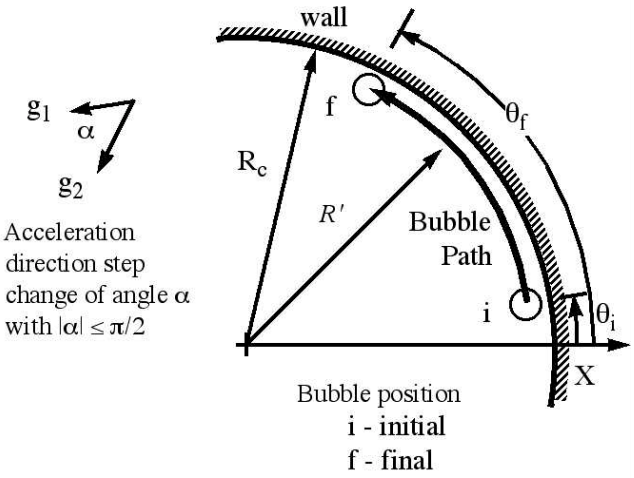

Figure 2: Bubble path for acceleration direction step changes between 0° and 90°.

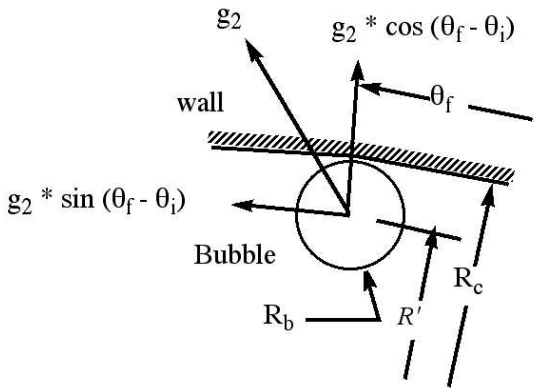

Figure 4: Acceleration levels applied while bubble is constrained by wall.

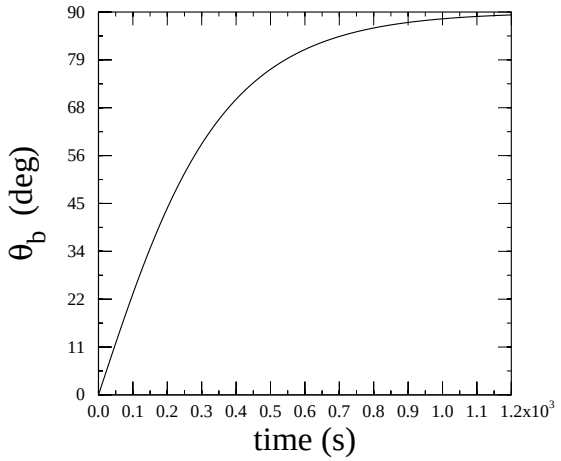

Figure 5: History of bubble's azimuthal position for $\theta_f - \theta_i = 90°$.

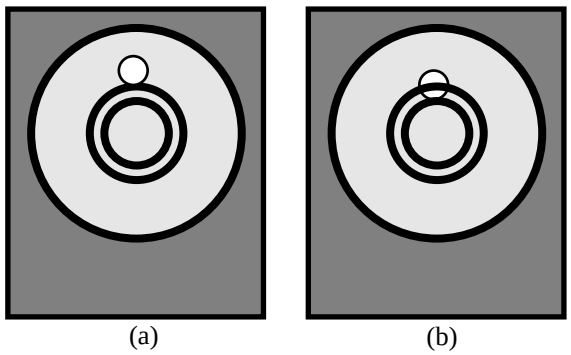

Figure 7: Bubble position in front (vertical plane) bubble level during (a) captive and (b) free-fall drops in the 2.2 second drop tower.

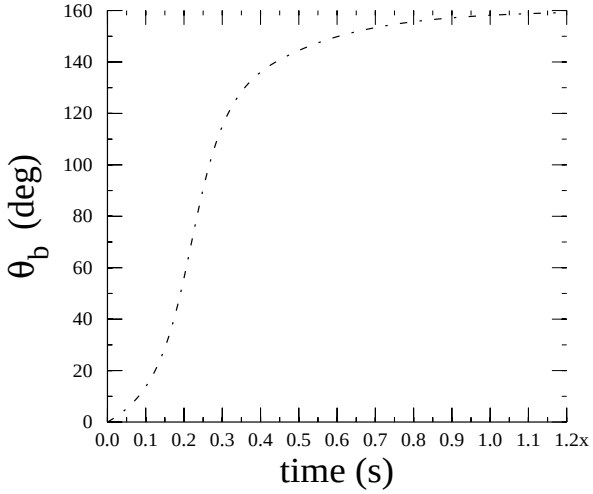

Figure 6: History of bubble's azimuthal position for $\theta_f - \theta_i = 160°$.

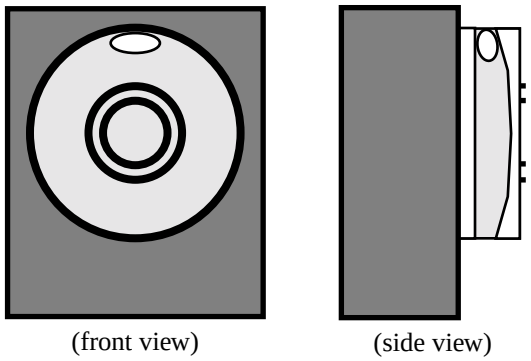

Figure 8: Bubble position in front (vertical plane) bubble level before drops in the 2.2 second drop tower at NASA Glenn Research Center.

REPORT DOCUMENTATION PAGE

Form Approved
OMB No. 0704-0188

1. AGENCY USE ONLY (*Leave blank*)	2. REPORT DATE	3. REPORT TYPE AND DATES COVERED
	May 2000	Technical Memorandum

4. TITLE AND SUBTITLE

Quasi-Steady Acceleration Direction Indicator in Three Dimensions

5. FUNDING NUMBERS

WU–398–95–0G–00

6. AUTHOR(S)

Richard DeLombard, Emily S. Nelson, and Kenol Jules

7. PERFORMING ORGANIZATION NAME(S) AND ADDRESS(ES)

National Aeronautics and Space Administration
John H. Glenn Research Center at Lewis Field
Cleveland, Ohio 44135–3191

8. PERFORMING ORGANIZATION REPORT NUMBER

E–12175

9. SPONSORING/MONITORING AGENCY NAME(S) AND ADDRESS(ES)

National Aeronautics and Space Administration
Washington, DC 20546–0001

10. SPONSORING/MONITORING AGENCY REPORT NUMBER

NASA TM—2000-209931
AIAA–2000–0570

11. SUPPLEMENTARY NOTES

Prepared for the 38th Aerospace Sciences Meeting and Exhibit sponsored by the American Institute of Aeronautics and Astronautics, Reno, Nevada, January 10–13, 2000. Responsible person, Richard DeLombard, organization code 6727, (216) 433–5285.

12a. DISTRIBUTION/AVAILABILITY STATEMENT

Unclassified - Unlimited
Subject Categories: 19 and 34 Distribution: Nonstandard

This publication is available from the NASA Center for AeroSpace Information, (301) 621–0390.

12b. DISTRIBUTION CODE

13. ABSTRACT ***(Maximum 200 words)***

Many materials processing and fluids physics experiments conducted in a microgravity environment require knowledge of the orientation of the low-frequency acceleration vector. This need becomes especially acute for space experiments such as directional solidification of a molten semiconductor, which is extremely sensitive to orientation and may involve tens of hours of operations of a materials furnace. These low-frequency acceleration data have been measured for many Shuttle missions with the Orbital Acceleration Research Experiment. Previous attempts at using fluid chambers for acceleration measurements have met with limited success due to pointing and vehicle attitude complications. An acceleration direction indicator is described, which is comprised of two orthogonal short cylinders of fluid, each with a small bubble. The motion and the position of the bubble within the chamber will indicate the direction of the acceleration experienced at the sensor location. The direction of the acceleration vector may then be calculated from these data. The frequency response of such an instrument may be tailored for particular experiments with the proper selection of fluid and gas parameters, surface type, and geometry. A three-dimensional system for sensing and displaying the low-frequency acceleration direction via an innovative technique described in this paper has advantages in terms of size, mass, and power compared with electronic instrumentation systems.

14. SUBJECT TERMS

Microgravity; Acceleration; Instrumentation

15. NUMBER OF PAGES

13

16. PRICE CODE

A03

17. SECURITY CLASSIFICATION OF REPORT	18. SECURITY CLASSIFICATION OF THIS PAGE	19. SECURITY CLASSIFICATION OF ABSTRACT	20. LIMITATION OF ABSTRACT
Unclassified	Unclassified	Unclassified	